

Electronic Supplementary Information

Efficient and reliable encapsulation for perovskite/silicon tandem solar modules

Francesco Toniolo,^{1,2,4} Helen Bristow¹, Maxime Babics,¹ Livia M. D. Loiola,³ Jiang Liu,¹ Ahmed Ali Said,¹ Lujia Xu,¹ Erkan Aydin,¹ Thomas Allen,¹ Moreno Meneghetti,² Suzana P. Nunes,³ Michele De Bastiani,^{1,3,4,*} Stefaan De Wolf^{1,*}

¹ KAUST Solar Center (KSC), Physical Sciences and Engineering Division (PSE), King Abdullah University of Science and Technology (KAUST), Thuwal 23955-6900, Kingdom of Saudi Arabia.

² Department of Chemical Science, Università degli Studi di Padova, Via F. Marzolo 1, 35131 Padova, Italy

³ Nanostructured Polymer Membrane Laboratory, Biological and Environmental Science and Engineering Division (BESE), King Abdullah University of Science and Technology (KAUST), Thuwal, 23955-6900, Saudi Arabia

⁴ current affiliation: Department of Chemistry & INSTM Università di Pavia, Via T. Taramelli 14, Pavia 27100, Italy.

*Email: michele.debastiani@kaust.edu.sa; stefaan.dewolf@kaust.edu.sa

1. Perovskite/Silicon Tandem Fabrication

Our c-Si bottom cell relies on silicon heterojunction technology,¹ for which 4-inch double-sided polished wafers (float-zone, TOPSIL, n-doped, resistivity 1–5 $\Omega\text{ cm}^{-1}$, and thickness 250–280 μm) were used as starting point. A randomly textured pyramid structure was then obtained using an alkaline solution. The texturing process was followed by a two-step solution-based cleaning procedure (RCA1 and RCA2). RCA1 is used to remove organic contaminants, by oxidation of the wafer surface in an $\text{NH}_4:\text{H}_2\text{O}_2:\text{H}_2\text{O}$ solution at 75°C. The RCA1 oxide layer is then removed in a dilute hydrofluoric acid (HF) solution at 5%. Following this, RCA2 is then used to remove metal contaminants, again by oxidation of the wafer surface in an $\text{HCl}:\text{H}_2\text{O}_2:\text{H}_2\text{O}$ solution at 75°C; this oxide is then again removed by a dilute HF solution. In between these steps, the wafers are rinsed thoroughly with DI water, followed by drying. After the wet chemical processing, the surfaces of the wafers were passivated by the deposition of intrinsic (i) hydrogenated amorphous silicon (a-Si:H) followed by deposition of doped amorphous and nanocrystalline layers (p and nc-n with a thickness of 12 and 40 nm, respectively) in a plasma enhanced chemical vapor deposition (PECVD) / physical vapor deposition (PVD) cluster (Octopus2, Indeotec). The deposition of these layers uses silane, phosphine, and trimethyl borane (TMB) as precursor gases.² To create the rear contact, indium-doped zirconium oxide (IZrO) and Ag films were

sputtered on the rear side (150nm and 250nm, respectively). At the front, for the recombination junction, 20 nm of indium tin oxide (ITO) was sputtered.

Once the silicon bottom cell is fabricated, the different perovskite top cell layers are deposited to construct the perovskite/silicon tandem. In this work, we opted for the so-called p-i-n configuration (also called inverted structure), resulting in a tandem device where the electron-collecting contact faces sunwards. As hole transport layer (HTL) for the perovskite, 2PACz [2-(9H-Carbazol-9-yl)ethyl]phosphonic acid (>98%, Tokyo chemical industry) has been used, which is a self assembled molecule (SAM), anchored on the top TCO of the silicon bottom cell, via spin coating at 5000 rpm for 50 seconds, followed by a drying step at 100°C for 10 minutes.³ The concentration precursor solution was 1mg/ml in ethanol. A UV-Ozone treatment for 900 seconds was carried out before the deposition. Subsequently, a 1.7M $\text{Cs}_{0.05}\text{FA}_{0.8}\text{MA}_{0.15}\text{Pb}(\text{I}_{0.75}\text{Br}_{0.25})_3$ perovskite precursor solution was prepared by dissolving a mixture of FAI (Greatcell solar), MABr (Greatcell solar), CsI (99.999% Sigma Aldrich), PbI_2 (99.999%, Alfa Aesar), and PbBr_2 (99.999% Alfa Aesar) in a mixed solvent DMF/DMSO 4:1. 75 μL of perovskite solution was spin-coated at 2,000 rpm for 45 s. After that, the speed was increased to 7,000 rpm for 8 s. Chlorobenzene was dropped on the substrates 12 s before the end of the spin-coating process. After the deposition, the substrates were annealed at 100°C for 15 minutes. The whole process is done in the nitrogen-filled glovebox. On top of the perovskite, 1 nm of lithium fluoride (LiF) (99.85%, Alfa Aesar) and 20nm of C_{60} (> 99.95% NanoC) were thermally evaporated (Angstrom Evovac). On top of this contact stack, 20 nm of SnO_x were then deposited by atomic layer deposition (ALD) using a Picosun system. The substrate temperature was maintained at 100°C during ALD deposition with tetrakis-dimethylamine tin (TDMA Sn) precursor source at 80°C and H_2O source at 18°C. 150 cycles were used to achieve the final thickness. For the IZO deposition, a 3-inch IZO ceramic target containing 98 wt% In_2O_3 and 2 wt% ZnO was used. Through a shadow mask, 75 nm of IZO was sputtered on top of the SnO_x . On top of the IZO layer, Ag fingers with a thickness of 350 nm were thermally evaporated using a high-precision magnetic shadow mask. The evaporation rate and thickness of each deposition were monitored by quartz crystal microbalance sensors.

As stated, the minimodule was obtained by sandwiching the tandem solar cell between two encapsulant sheets and two standard module glasses with a dimension of 7 x 7 cm² and 3.2 mm in thickness. First, to enable electrical characterization, the contacts need to be extracted from the minimodule, and this has been done via the so-called tabbing process. In particular, two copper ribbons, covered with a Pb/Sn alloy are placed on the top and bottom contacts utilizing a silver paste. To ensure a proper connection and eliminate the solvents present in the silver paste, thermal annealing at 120°C under a mild vacuum for 10 minutes has been carried out. The encapsulations were done using an industrial vacuum laminator (Ecolam 5, Ecoprogetti). To secure the edges of the modules and to avoid moisture ingress through the tabbing we used a double layer of edge sealant (poly isobutylene, PIB, butyl rubber) on the sides of the glass. Finally, the layer stack was placed inside the laminator and encapsulated at 120°C when TPU was adopted or 110°C in the case

of TPO. TPU has been purchased from the company Swmintl (<https://www.swmintl.com/>) while TPO has been purchased from the company Borealis (<https://www.borealisgroup.com/>).

2. Tandem Characterization (Solar simulator, EQE, climate chamber)

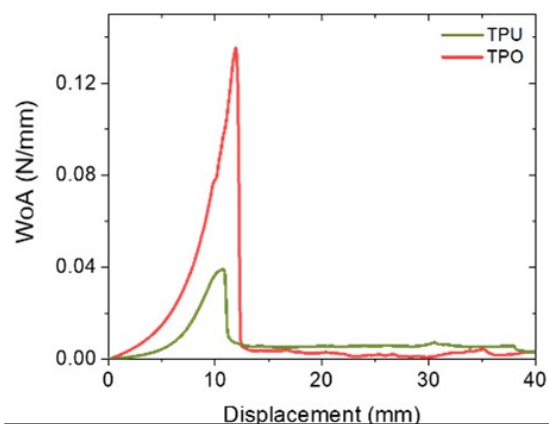
Once the tandem devices were fabricated, their J-V characteristic curves were collected before and after encapsulation. To do this, a Wavelabs Sinus 220 LED-based solar simulator with AM1.5G irradiance spectrum was used as a light source, coupled with a Keithley 2400 series SourceMeter. The devices were measured with a voltage sweep from -0.1 V to +1.9 V in forward and reverse scan directions with 10 mV of step-voltage and 100 mV/s scan rate, under dark and illumination conditions. The device's active area was defined with a laser-cut shadow mask, with an aperture of 1 cm². The light intensity was calibrated using Fraunhofer ISE Callab certified c-Si solar cells.

External quantum efficiency (EQE) measurements were collected using a LOANA system (PV-Tools). The chopped monochromatic light beam was focused on the active area of the solar cell, avoiding the silver fingers. Two bias lights were employed. A near-infrared LED (950 nm) and a green LED light (525 nm) were used to saturate the silicon or perovskite sub-cell responses, respectively, to measure the complementary cell's EQE. In addition, 0.6V bias voltage was applied to isolate the current response.

3. Mechanical, Thermal and Thermomechanical Analyzes

Peel Testing

The work of adhesion (WoA) was evaluated using a Yeonjin TXA texture analyzer. The partially encapsulated samples were fixed on glass slides and mounted in a 180° configuration. The dimensions of the sample are 2.1x2.1 cm. The adhesion of the adhesive tape is calibrated on a reference glass slide. The samples are glued



on a glass holder during the measurements.

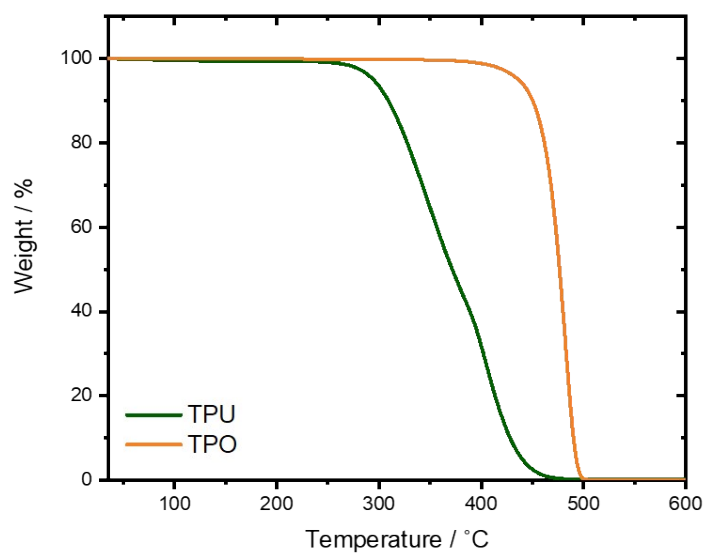
Supplementary Figure 1 | Work of adhesion of the encapsulants on the tandem solar cell top surface.

Stress versus strain curves

The mechanical properties of cured TPO and TPU films were investigated using a Discovery DMA850 from TA Instruments at 25°C at a rate control stress ramp test mode, and using a tensile film clamp set-up. An initial pre-load force of 0.01 N was applied, and it increased at the ramp rate of 0.5 N min⁻¹ until the maximum force of 18.0 N. Homogeneous specimens were used for the mechanical tests, and they presented thickness of about (0.385 ± 0.007) mm for TPO and (0.66 ± 0.02) mm for TPU, width of about 5.8-6.4 mm, and length (gap) of 10 mm. The elastic moduli of the materials were calculated using the TRIOS Guardian software, and the average of the multiple curves (N = 5) and standard errors were calculated using OriginPro.

Thermogravimetric Analysis

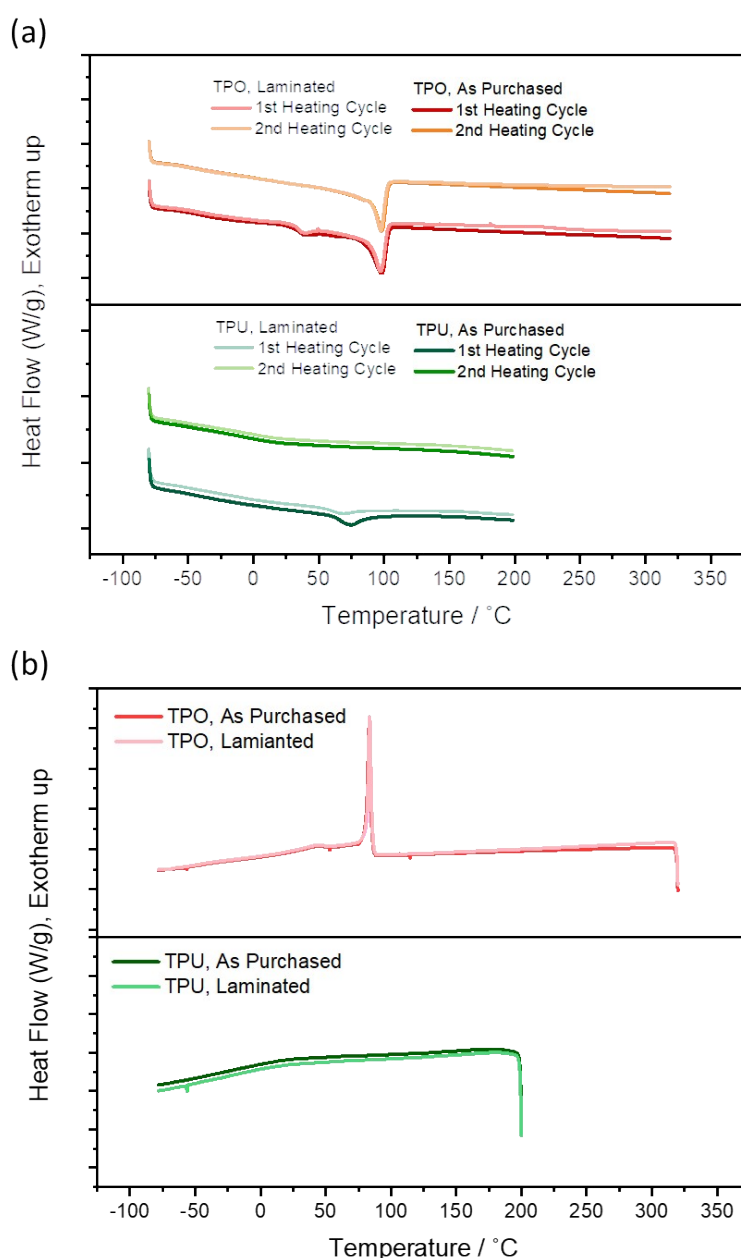
The thermal stability of the as purchased TPO and TPU materials was investigated using a Discovery TGA system. Thermogravimetric analysis (TGA) was performed with a ramp rate of $10\text{ }^{\circ}\text{C min}^{-1}$.



Supplementary Figure 2 | Thermogravimetric Analysis (TGA) of the as purchased TPO and TPU-based materials. Used to define the upper temperature limit of the DSC measurements.

Differential Scanning Calorimetry

The thermal transitions of the as purchased as well as cured TPO and TPU materials were investigated using a Discovery DSC system. Samples of mass 6-9 mg were loaded in aluminium TZero pans for the measurements. Differential scanning calorimetry (DSC) scans were performed with a ramp rate of $10\text{ }^{\circ}\text{C min}^{-1}$. Before the first heating cycle the sample was cooled from room temperature to $-80\text{ }^{\circ}\text{C}$, which took around 2 minutes. The upper limit of the DSC was defined based on the TGA of the two materials.



Supplementary Figure 3 | Differential scanning calorimetry (DSC) of the as purchased and laminated TPO and TPU –based materials (a) first and second heating cycles and (b) cooling cycles.

	T_g DSC 2 nd heating (°C)	T_g DMA E'' versus T (°C)	T_c DSC cooling (°C)	T_m DSC 2 nd heating (°C)
Cured TPU	-31	-29	-	-
Cured TPO	-45	-39	83	98

Supplementary Table 1 | Glass transition (T_g), crystallization and melt temperatures for the vacuum-laminated (cured) TPU and TPO-based materials determined from differential scanning calorimetry (DSC) and dynamic mechanical thermal analysis (DMA).

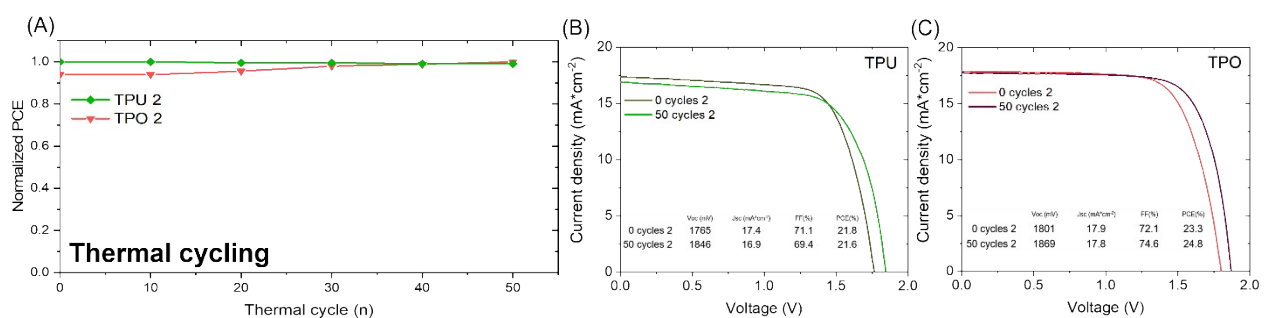
Dynamic Mechanical Analyzes

Dynamic mechanical analyzes were performed on a DMA850 from TA Instruments applying an initial preload force of 0.01 N, using a tensile film clamp set-up in an oscillation mode (frequency of 1 Hz and 20 μ m of amplitude). The homogeneous specimens presented thickness of about (0.385 \pm 0.007) mm for TPO and (0.66 \pm 0.02) mm for TPU, width of about 5.8-6.4 mm, and length (gap) of 10 mm were used for the tests. The dynamic mechanical properties of the films were recorded during the temperature ramp at 2°C min⁻¹ from -90°C to 100°C (after conditioning the samples at -90°C for 30 minutes).

4. Stability tests

Thermal cycling

For the stability tests, an environmental climate chamber was used (Weiss Technik). In order to perform the TC test, the devices were placed inside the chamber and the temperature was varied from +85°C to -40°C, keeping the maximum temperature ramp below the 100°C/h threshold.⁴ The devices were taken out for J-V

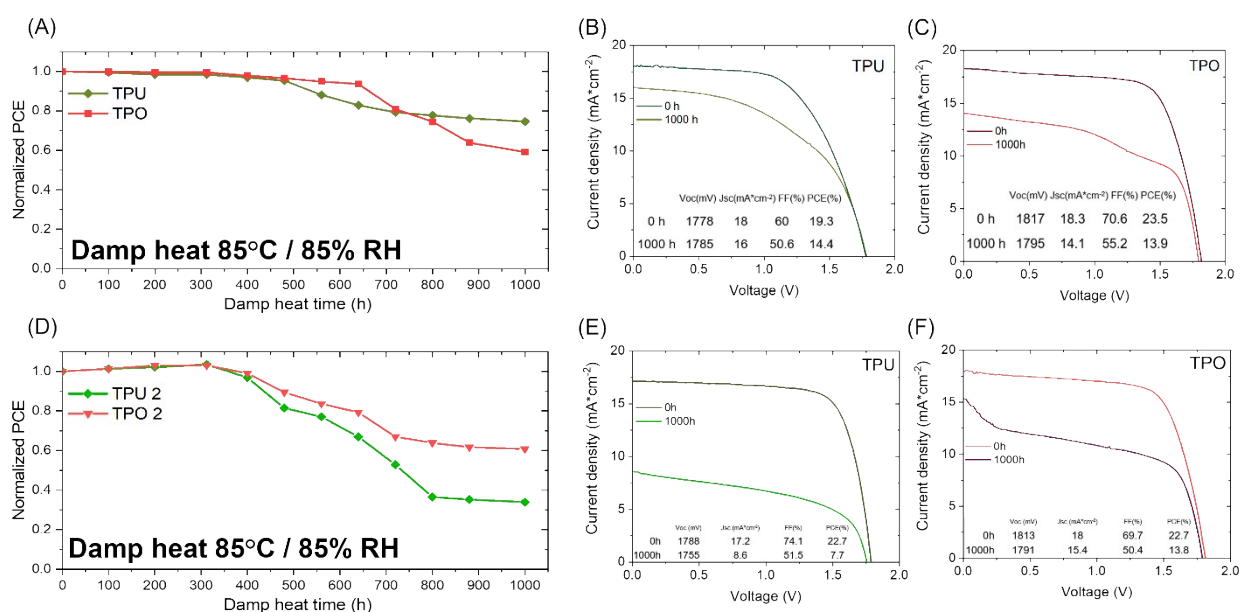


measurements at some intervals.

Supplementary Figure 4 | (A) Additional thermal cycle and comparison between the J-V curves before and after the TC test in the case of two minimodules encapsulated with TPU (B) and TPO (C).

Damp heat

The same procedure was adopted for the damp-heat test, but in this case, the environmental condition was set and kept at 85°C and 85% RH for 1000h. Tandems encapsulated with both TPO and TPU were also exposed to 1000 hours of damp-heat testing, at 85 °C an 85% relative humidity as mandated by the IEC61215 standard. The observed PCE trends of the DH test clearly show that the minimodules lost performance over time, particularly after 400-500 h of testing. After the test, the minimodule sealed with TPU retained almost 80% of the initial performance, while the minimodule sealed with TPO retained only 60% of the initial performance. We attribute these losses to the degradation of the tandem devices, with a mechanism that is independent of the encapsulation strategy. Indeed, similar trends in stability were observed by Liu et al. and attributed to increasing charge recombination at the perovskite/fullerene interface, particularly when LiF was adopted as interlayer and after 400 h of the DH test.⁵ Replacing the LiF interlayer with MgF₂ improved significantly the performance in the DH test, confirming that the degradation is happening within the device



and not due to a failure of the encapsulation.

Supplementary Figure 5 | Power conversion efficiency trend during 1000h of DH test for two different sets of samples (A) and (D). Figures (B), (C), (E) and (F) show the comparison between the J-V curves before and after the DH test in the case of the tested minimodules encapsulated with TPU (B and E) and TPO (C and F).

References

1. Razzaq, A., Allen, T. G., Liu, W., Liu, Z. & de Wolf, S. Silicon heterojunction solar cells: Techno-economic assessment and opportunities. *Joule* **6**, 514–542 (2022).
2. Hou, Y. *et al.* Efficient tandem solar cells with solution-processed perovskite on textured crystalline silicon. *Science (1979)* **367**, 1135–1140 (2020).
3. Al-Ashouri, A. *et al.* Conformal monolayer contacts with lossless interfaces for perovskite single junction and monolithic tandem solar cells. *Energy Environ Sci* **12**, 3356–3369 (2019).
4. Holzhey, P. & Saliba, M. A full overview of international standards assessing the long-term stability of perovskite solar cells. *J Mater Chem A Mater* **6**, 21794–21808 (2018).
5. Liu, J. *et al.* Efficient and stable perovskite-silicon tandem solar cells through contact displacement by MgFx. *Science (1979)* **377**, 302–306 (2022).